Plasticity of astroglial networks in olfactory glomeruli

Lisa Roux[a,b,c], Karim Benchenane[d], Jeffrey D. Rothstein[e], Gilles Bonvento[f,g], and Christian Giaume[a,b,c,1]

[a]Collège de France, Center for Interdisciplinary Research in Biology (CIRB)/Centre National de la Recherche Scientifique, Unité Mixte de Recherche 7241/Institut National de la Santé et de la Recherche Médicale U1050, 75231 Paris Cedex 05, France; [b]University Pierre et Marie Curie, ED, N°158, 75005 Paris, France; [c]MEMOLIFE Laboratory of Excellence and Paris Science Lettre Research University, 75005 Paris, France; [d]Unité Mixte de Recherche 7102, Centre National de la Recherche Scientifique, Laboratoire Neurobiologie des Processus Adaptatifs, Navigation, Mémoire et Vieillissement, Université Pierre et Marie Curie, 75005 Paris, France; [e]Department of Neurology, Johns Hopkins University School of Medicine, Baltimore, MD 21205; [f]Commissariat à l'Energie Atomique, Institute of Biomedical Imaging (I2BM), Molecular Imaging Research Center, 92265 Fontenay-aux-Roses Cedex, France; and [g]Unité de Recherche Associée 2210, Centre National de la Recherche Scientifique, Commissariat à l'Energie Atomique, 92265 Fontenay-aux-Roses Cedex, France

Edited by Michael V. L. Bennett, Albert Einstein College of Medicine, Bronx, NY, and approved September 15, 2011 (received for review May 13, 2011)

Several recent findings have shown that neurons as well as astrocytes are organized into networks. Indeed, astrocytes are interconnected through connexin-formed gap junction channels allowing exchanges of ions and signaling molecules. The aim of this study is to characterize astrocyte network properties in mouse olfactory glomeruli where neuronal connectivity is highly ordered. Dye-coupling experiments performed in olfactory bulb acute slices (P16–P22) highlight a preferential communication between astrocytes within glomeruli and not between astrocytes in adjacent glomeruli. Such organization relies on the oriented morphology of glomerular astrocytes to the glomerulus center and the enriched expression of two astroglial connexins (Cx43 and Cx30) within the glomeruli. Glomerular astrocytes detect neuronal activity showing membrane potential fluctuations correlated with glomerular local field potentials. Accordingly, gap junctional coupling of glomerular networks is reduced when neuronal activity is silenced by TTX treatment or after early sensory deprivation. Such modulation is lost in Cx30 but not in Cx43 KO mice, indicating that Cx30-formed channels are the molecular targets of this activity-dependent modulation. Extracellular potassium is a key player in this neuroglial interaction, because (*i*) the inhibition of dye coupling observed in the presence of TTX or after sensory deprivation is restored by increasing $[K^+]_e$ and (*ii*) treatment with a K_{ir} channel blocker inhibits dye spread between glomerular astrocytes. Together, these results demonstrate that extracellular potassium generated by neuronal activity modulates Cx30-mediated gap junctional communication between glomerular astrocytes, indicating that strong neuroglial interactions take place at this first relay of olfactory information processing.

glia | functional unit | naris occlusion

Olfactory glomeruli (OG) represent functional units where olfactory signals are first processed (1, 2). The combination of the anatomical organization and the functional activity results in a highly ordered spatial map of glomerular activation associated with each odor (3, 4). However, this well-described organization refers only to neuronal circuits, and information concerning astroglial connectivity is lacking. In the brain, astrocytes express the highest rate of connexins (Cxs), the protein constituents of gap junction channels that provide the molecular basis for direct cell-to-cell communication. Though astrocytes were initially thought to form a glial syncitium, there is now evidence for a more specialized network organization (5). As increasing evidence argues for dynamic interactions between neurons and astrocytes (6), a coordinated population of astrocytes working in concert with neurons could contribute to sensory integration occurring in OG. The goal of this study is to determine how Cx-mediated intercellular communication in astrocytes is organized and modulated in this brain structure characterized by functional units. Features of OG astrocytes studied so far include their morphology (7, 8), membrane currents (9, 10), and contribution to hemodynamic responses (11–13). Here, we report that in the glomerular layer (GL), astroglial morphologies and Cx expression patterns lead to a gap junctional communication (GJC) favored within individual OG. Importantly, this study also demonstrates that extracellular potassium generated by neuronal activity locally modulates Cx30-mediated GJC between glomerular astrocytes, indicating that activity-dependent neuroglial interactions occur within these functional units.

Results

Astroglial Network Organization in the Glomerular Layer. OG consist of bundles of fibers and synapses (neuropile) delimited by periglomerular cell bodies. Among them, glomerular astrocytes (OG astrocytes) have a cell body in direct contact with this neuropile (7). The human glial fibrillary acidic protein (hGFAP)/EGFP mouse strain (14) allowed studying the morphology of isolated GFP^+ astrocytes, because all astrocytes are not labeled in this model (Fig. 1*A* and *SI Appendix*, *SI Methods*). Although a minority of the analyzed OG astrocytes (3 of 16) sent one process in an adjacent glomerulus, 90 ± 4% of primary processes were located within OG neuropile ($n = 44$). The averaged vector representing the primary processes of each astrocyte formed an angle of 29 ± 10° ($n = 14$) with the vector drawn between the soma and the OG center (*SI Appendix*, *SI Methods*). In addition, anti-GFP immunofluorescence originating from OG astrocyte processes mostly remained within OG (85 ± 6% of the total fluorescence measured on cell processes, $n = 4$ isolated cells; Fig. 1*A*). As a whole, this quantitative analysis shows that the morphology of OG astrocytes is intimately associated with a single OG.

Cx expression was studied by immunohistochemistry at different scales: on low-magnification images of the GL (*SI Appendix*, Fig. S1) and, more precisely, at the level of glomerular boundaries (Fig. 1*D* and *SI Appendix*, *SI Methods*). Both astroglial Cxs, Cx43 and Cx30, were enriched within OG compared with the extraglomerular area (Fig. 1 *B–D* and *SI Appendix*, Fig. S1). The differential of expression between these two regions was significantly higher for Cx30 than for Cx43 (Fig. 1*D*). In addition, within OG, Cx43 expression was favored at the edge of the neuropile, and Cx30 expression also increased toward the center (Fig. 1*D* and *SI Appendix*, Fig. S2).

Dye-coupling experiments were performed in acute olfactory bulb (OB) slices (P15–P25) by dialyzing an astrocyte recorded in the whole-cell configuration with sulforhodamin B (SrB), a gap junction channel-permeant dye. Patch-clamp recordings in the GL allowed identification of astrocytes by their membrane potential (V_m; −79.8 ± 0.3 mV, $n = 136$) and their linear I–V relationship. The number of dye-coupled cells observed after 20 min of dialysis of an OG astrocyte averaged 76 ± 3 cells ($n = 26$). To study in more detail the spatial organization of astroglial coupling, we used

Author contributions: L.R., G.B., and C.G. designed research; L.R. performed research; K.B. and J.D.R. contributed new reagents/analytic tools; L.R. and K.B. analyzed data; and L.R., K.B., G.B., and C.G. wrote the paper.

The authors declare no conflict of interest.

This article is a PNAS Direct Submission.

[1]To whom correspondence should be addressed. E-mail: giaume@college-de-france.fr.

This article contains supporting information online at www.pnas.org/lookup/suppl/doi:10.1073/pnas.1107386108/-/DCSupplemental.

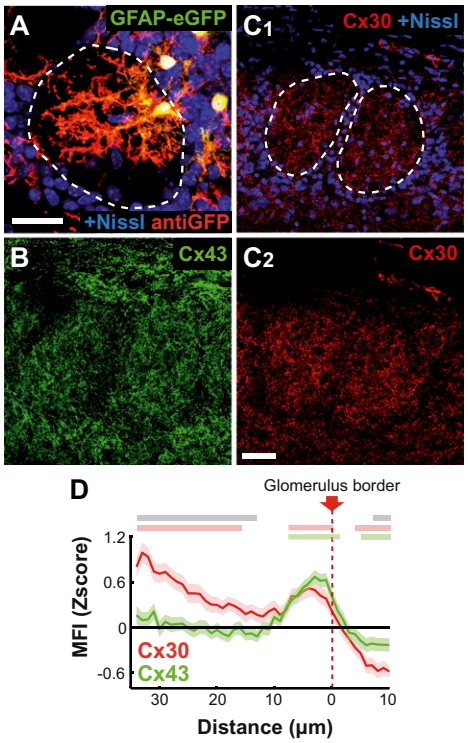

Fig. 1. Compartmentalized astrocyte morphology and connexin expression in the glomerular layer. (*A*) Typical morphology of glomerular astrocytes observed at P20 in hGFAP/EGFP mice. Glomerular boundaries (dotted line) are defined by a Nissl staining (blue). Amplification provided by anti-GFP antibodies reveals fine astrocytic processes that are mostly located within OG. (Scale bar: 25 µm.) (*B* and *C*) Cx30 (*C*; red) and Cx43 (*B*; green) immunoreactivity was studied in the GL at P20 on single confocal sections. (*B*) Example of Cx43 immunostaining. (*C1* and *C2*) Example of Cx30 immunostaining with (*C1*) or without (*C2*) Nissl staining (blue). Nissl-defined OG borders are indicated by dotted lines in *C1*. (Scale bar: 30 µm.) (*D*) Quantitative analysis of mean fluorescence intensity (MFI) for Cx43 (green) and Cx30 (red) immunostainings at the OG border, performed on 109 and 67 OG, respectively (SEM are indicated by light colors surrounding curves) (*SI Appendix, SI Methods*). To combine data obtained from different experiments, results were expressed in *Z* scores. Horizontal gray lines above the graph correspond to significant difference between the two Cx levels of expression ($P < 0.05$). Horizontal green and red lines indicate an expression significantly different from the mean for Cx43 and Cx30, respectively. Note the significant decrease in Cx expression measured outside OG compared with the glomerular area ($P < 0.01$ and $P < 0.001$ for Cx43 and Cx30, respectively). This differential expression was significantly larger for Cx30 than Cx43 ($P < 0.001$, two-way ANOVA).

the glutamate transporter-1 (GLT-1)/EGFP BAC reporter mice (15), in which most astrocytes are GFP^+. Indeed, in the GL, GFAP and S100 immunoreactivity was detected in most of the GFP^+ cells, whereas GFP never colocalized with NeuN or NG2 immunoreactivity (*SI Appendix*, Fig. S3). After injection in a single astrocyte and postfixation (*SI Appendix, SI Methods*), 93 ± 2% of SrB^+ cells were also GFP^+ ($n = 12$ injections; $n = 306$ cells; Fig. 2*A1*), indicating that astrocytes are mainly coupled to astrocytes. Interestingly, these reporter mice allowed us to visualize all GFP^+ candidates around the injected cell that could potentially receive the dye. The location [in the injected OG (Inj) or in adjacent OGs (Adj)] and distance to the injected cell was determined for each candidate, and a similar analysis was performed for all SrB^+-coupled cells (*SI Appendix, SI Methods*). When injection was carried out in glomerular astrocytes, a preferential GJC between astrocytes located in the same OG was observed ($P < 0.01$; Fig. 2 *A1* and *A2*), regardless of the distance from the injected cell considered (Fig. 2*B*). As a whole, 76 ± 6% of the coupled cells belonged to the injected OG, whereas only 16 ± 5% were located

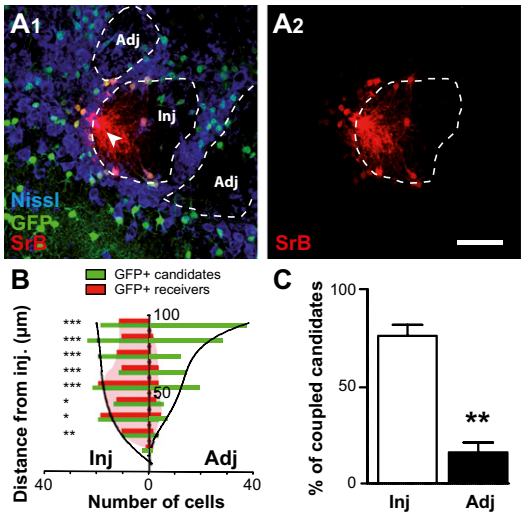

Fig. 2. Astroglial networks are confined within glomeruli. (*A1* and *A2*) Injections of sulforhodamine B (SrB, red) were performed in glomerular astrocytes from GLT-1/EGFP BAC reporter mice in which astrocytes that could potentially receive the dye were visualized (green in *A1*). 3D confocal analysis of SrB^+ and GFP^+ astrocytes, associated with a Nissl staining (blue) to define OG limits, allowed us to determine the distance of SrB^+ and GFP^+ cells from the injected cell (arrow), taking into account their location [within the injected glomerulus (Inj) or in adjacent OG (Adj)]. Examples illustrated in *A1* and *A2* were obtained from projections of 12 confocal planes (1 µm each). (Scale bar: 50 µm.) (*B*) For each location (Inj or Adj), the number of GFP^+ (green) and SrB^+ (red) cells was obtained for a defined range of distances from the injection site (10-µm large concentric rings from 0–10 to 90–100 µm). Results obtained from six injections were pooled (*SI Appendix, SI Methods*) and indicate a preferential dye coupling between astrocytes from the same OG. χ^2 tests were applied for each distance, to compare the percentage of coupled candidates between the two locations (Inj or Adj). $*P < 0.05$, $**P < 0.01$, and $***P < 0.001$. (*C*) The number of GFP^+ astrocytes located either in the injected or in an adjacent OG was determined within a fixed volume around the injected cell (*SI Appendix, SI Methods*). Within the injected OG, 76 ± 6% of these potential "receiver" cells for the dye are coupled, whereas only 16 ± 5% of the astrocytes located in adjacent OG receive the dye ($n = 6$ injections, $**P < 0.01$, χ^2 test; see *SI Appendix*, Fig. S5 for complementary information).

in adjacent OGs ($n = 6$ injections; $n = 105$ and 87 cells for Inj and Adj, respectively; Fig. 2*C* and *SI Appendix*, Fig. S4). Together, these observations suggest that glomerular astroglial networks respect the organization in discrete units present in the GL.

Neuronal Activity Modulates GJC Between Glomerular Astrocytes. We found that astrocyte V_m recorded in the GL during dye-coupling experiments showed small but consistent fluctuations (in the range of 0.05–0.2 Hz) with an amplitude defined as V_m SD (see ref. 16) averaging 0.5 ± 0.05 mV ($n = 118$; Fig. 3 *B* and *C*). These fluctuations were abolished in presence of 0.5 µM TTX (Fig. 3*C*) and highly correlated with local field potentials (LFP) recorded in the same OG (Fig. 3 *C* and *D* and *SI Appendix*, Fig. S5). Indeed, for 18 analyzed recordings, significant correlation with the LFP was detected by cross-correlogram analysis (zero-lag correlation, $r = -0.45 \pm 0.05$; $P < 0.001$ for each cell; *SI Appendix*, Fig. S5 and *SI Methods*). On average, astrocyte activity was delayed by 722 ± 143 ms compared with the LFP (Fig. 3*D* and *SI Appendix*, Fig. S6). LFP signals could result from the already described synchronized activity of the mitral/tufted cells (M/TCs) projecting to the same OG (17, 18). Together, these data demonstrate that within OG, astrocytes detect neuronal activity.

This property associated with the enriched expression of Cxs within OG led us to question whether neuronal activity modulates glomerular networks. Following TTX treatment (0.5 µM, 1–3 h), the number of coupled cells was significantly reduced by 43% (Fig.

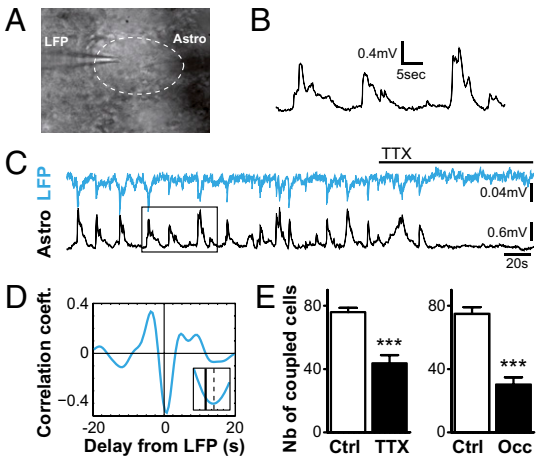

Fig. 3. Astrocyte GJC is regulated by neuronal activity within olfactory glomeruli. (*A*) Typical IR-differential interference contrast image of simultaneous recordings of local field potential (LFP) and V_m of glomerular astrocyte in the same glomerulus (delimited by dotted line) with the two recording pipettes. (*B*) V_m in glomerular astrocytes show fluctuations as indicated by whole-cell recordings. (*C*) Simultaneous recordings of LFP (blue) and astrocyte V_m (black) in the same glomerulus showed correlated fluctuations (zero-lag correlation, $r = -0.7$, $P < 0.01$; see cross-correlogram analysis in *SI Appendix*, Fig. S5) silenced in presence of 0.5 μM TTX (horizontal bar). Rectangle shows the region presented in *B*. (*D*) Averaged cross-correlogram obtained for 18 recordings, filtered in the 0.05- to 0.2-Hz frequency band, showed similar correlation ($r = -0.45 \pm 0.05$, $P < 0.01$). The lag corresponding to the maximal negative value of the correlation coefficient (indicated by dotted line in the *Inset*) indicates that astrocyte V_m is delayed by 722 ± 143 ms compared with LFP. (*Inset*) High magnification of the curve around zero lag (*SI Appendix*, Fig. S5). (*E Left*) For dye injections in OG astrocytes, treatment with TTX resulted in a significant reduction of dye coupling (n = 26 and 12 in control and TTX conditions, respectively; $P < 0.0001$). (*E Right*) Unilateral naris occlusion (Occ) performed at P1 led to a reduced GJC at P20 between glomerular astrocytes (n = 11 and 12 for control and occluded conditions, respectively; $P < 0.0001$).

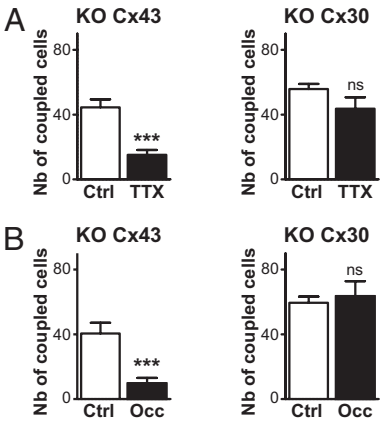

Fig. 4. Cx30 is the molecular target for the activity dependence of GJC between glomerular astrocytes. (*A*) In KO Cx43 mice, dye coupling was diminished by 66% in the presence of TTX when injections were performed in glomerular astrocytes (n = 6 for both control and TTX conditions; $P < 0.001$), whereas in KO Cx30 animals, dye coupling was not affected by TTX treatment (78% of control, n = 10 and n = 6 for control and TTX conditions, respectively; $P = 0.1462$). Note that in the control condition, the number of coupled cells was reduced by 42% (n = 6, $P < 0.001$) and 29% (n = 10, $P < 0.001$) in KO Cx43 and KO Cx30 mice, respectively, compared with wild type (n = 26). (*B*) Dye coupling was also strongly inhibited by early olfactory deprivation in P20 KO Cx43 mice (n = 4 and n = 5 for control and occluded conditions, respectively; $P < 0.01$), whereas in P20 KO Cx30 animals, dye coupling at P20 was not affected by olfactory deprivation (n = 4 and 5 for control and occluded conditions, respectively; $P = 0.72$).

3*E Left*). This effect was reversed after a 2-h wash (*SI Appendix*, Fig. S6)—the minimal delay to observe recovery of neuronal spiking in M/TCs (n = 3). To confirm the activity dependence of glomerular networks, an in vivo model of reduced neuronal activity was used. Unilateral naris occlusion carried out at P1 prevents stimuli from afferent olfactory sensory neurons and reduces MCs activity in the occluded OB (19). Occlusion efficiency was confirmed by the decreased size of the deprived OB compared with the contralateral one, and by the reduced tyrosine hydroxylase immunostaining performed postrecording (20) (*SI Appendix*, Fig. S8). Twenty days after sensory deprivation, dye coupling between OG astrocytes was significantly inhibited by 56% (Fig. 3*E Right*). Overall, these results demonstrate that communication between astrocytes is modulated by neuronal activity within OG.

Mechanism Targeting Cx30-Formed Channels and Involving Extracellular Potassium. The different expression patterns of the two astroglial Cxs within OG raises the question about possible differences in their physiological function. Knockout (KO) mice were used to identify the molecular target of the modulation exerted by neuronal activity on glomerular astroglial GJC. The lack of dye coupling in OB acute slices prepared from double-KO mice [$Cx30^{(-/-)}Cx43^{(fl/fl)}$:GFAP-cre] demonstrated that GJC in astrocytes is mainly mediated by Cx43 and Cx30 (n = 4). In presence of TTX, the extent of the dye coupling for glomerular injections was reduced by 66% in $Cx43^{(fl/fl)}$:GFAP-cre mice (KO Cx43) slices. In contrast, TTX had no effect in slices from KO Cx30 (Fig. 4*A*). Because the neuronal firing rate of MCs was similar in WT and KO Cx30 (1.2 ± 0.4 Hz, n = 10 and 1.4 ± 0.5 Hz, n = 9, respectively), the lack of TTX effect in the KO Cx30 cannot be attributed to reduced neuronal spiking activity. Hence, these data indicate that the activity dependence of astroglial glomerular networks relies on the regulation of Cx30 gap junction channels. To strengthen this statement, early sensory deprivations were performed in KO mice. Twenty days of sensory deprivation resulted in a 76% reduction of dye coupling in KO Cx43 mice, whereas the number of coupled cells in deprived OBs was not significantly different from control in KO Cx30 animals (Fig. 4*B*), in striking accordance with TTX application in slices. This specificity was reinforced by experiments performed in WT mice at P10, a developmental stage at which Cx30 is not expressed in astrocytes yet (21). At this age, like in KO Cx30, no inhibition of glomerular astroglial GJC was observed when TTX was applied (94% of control, n = 7 and 5, in control and TTX conditions, respectively; $P = 0.68$) or after sensory deprivation (92% of control, n = 7 and 4, in control and occlusion conditions, respectively; $P = 0.29$). More precisely, when dye coupling was tested at different time intervals after naris occlusion, sensory-deprived OBs showed a coupling similar to controls at postnatal day 10 (P10) and P15 (92%, n = 4, $P = 0.29$, and 99%, n = 7, $P = 0.45$, respectively) before the reduction observed at P20 (*SI Appendix*, Fig. S8). This time schedule corresponds to the appearance of Cx30 in the GL (n = 3) and confirms that Cx30 is the molecular substrate for the activity dependence of glomerular astroglial networks. These properties were not attributed to a reduction in Cx30 expression, because no change in Cx30 protein levels was detected after TTX treatment and naris occlusion by immunoblotting (*SI Appendix*, Fig. S8).

So far, V_m fluctuations in astrocytes have mostly been reported from in vivo experiments (16, 22) and have reflected changes in extracellular K^+ concentration ($[K^+]_e$) directly linked to neuronal activity. Because extracellular K^+ can regulate astroglial GJC (23, 24), changes in $[K^+]_e$ were hypothesized to play a role in the activity-dependent modulation of glomerular astrocyte GJC. Accordingly, a 3-mM increase in $[K^+]_e$ restored the dye

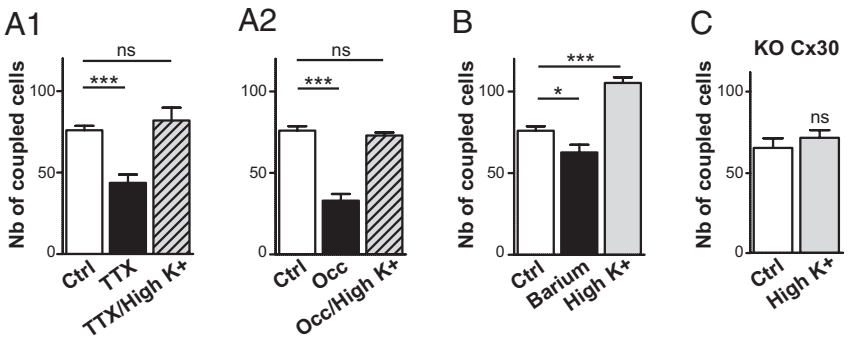

Fig. 5. The activity dependence of glomerular astroglial involves extracellular potassium. (*A1* and *A2*) For glomerular injections, dye-coupling inhibition by TTX treatment (43%, $n = 26$ and 12 in control and TTX conditions, respectively; $P < 0.0001$) and by early unilateral naris occlusion (56% inhibition, $n = 11$ and 12 for control and occluded conditions, respectively; $P < 0.0001$) was reversed in the presence of high $[K^+]_e$ (6 instead of 3 mM in control; 108% of control, $n = 6$, $P = 0.42$ and 96% of control, $n = 5$, $P = 0.67$, for TTX and occlusion, respectively). (*B*) Treatment with barium 200 μM decreased by 17% ($n = 6$, $P < 0.05$) the number of coupled cells, whereas this parameter was increased by 39% ($n = 4$, $P < 0.001$) in high $[K^+]_e$. (*C*) In contrast, high $[K^+]_e$ had no effect in KO Cx30 mouse (110% of control, $n = 8$, $P = 0.44$).

coupling level in the presence of TTX (Fig. 5*A1*) as well as after 20 d of sensory deprivation (Fig. 5*A2*). Such facilitating effect was also observed in absence of TTX (Fig. 5*B*), in a reversible manner (*SI Appendix*, Fig. S7), indicating that dye coupling in OG can be increased in basal condition. Importantly, blockade of K_{ir} channels with 200 μM of barium significantly reduced GJC between glomerular astrocytes by 17% (Fig. 5*B*), although neuronal activity was strongly increased (36.4 ± 4.3 Hz, $n = 4$, compared with 1.2 ± 0.4 Hz in control condition, $n = 10$; $P < 0.0001$). This finding demonstrates that the modulation of astroglial GJC by neuronal activity is partly dependent on K_{ir} channel function in astrocytes. Importantly, in the KO Cx30 mice where astroglial GJC was insensitive to TTX treatment, a 3-mM increase in $[K^+]_e$ was unable to increase the level of coupling (Fig. 5*C*). Together, these results indicate that extracellular K^+ generated by neuronal activity can modulate Cx30-mediated GJC between glomerular astrocytes via a mechanism involving K_{ir} channels.

Discussion

This study provides evidence that astroglial networks are compartmentalized in the olfactory GL, and that GJC within OG can be modulated by neuronal activity. These observations strongly challenge the well-known idea of a glial syncitium, and suggest an active role for these astroglial networks in olfactory information processing.

Astroglial Networking Respects the Glomerular Organization. In the GL, GJC between astrocytes is preferentially confined within OG and thus overlaps neuronal organization. This feature results from at least two astroglial properties: (*i*) the oriented morphology of glomerular astrocytes processes toward the OG center (7–9) where most of the GL neuronal transmission occurs, and (*ii*) the enriched expression of the two astroglial Cxs within functional units, as already reported in the somatosensory cortex (25). In addition, the physical barrier formed by the somata of the juxtaglomerular neurons can also contribute to the gap in Cx expression observed around glomeruli (Fig. 1*D*) and to the coupling confinement within OG. This phenomenon has already been observed in the hippocampus at the level of the pyramidal cell layer (26). Together, these properties indicate a certain degree of independence of each OG in terms of astroglial GJC that could restrain transfer of information between OGs and contribute to the accuracy of the glomerular map.

Neurons Set the Tone of Astroglial Networks. The inhibition of GJC following TTX treatment substantiates previous work showing that neuronal activity increases coupling in the intact optic nerve (27) and in astrocytes cocultured with neurons (28). We also show that early olfactory deprivation reduces GJC in astroglial glomerular networks. Recently, Maher et al. (29) reported that the function of Cx36-formed GJ channels in MCs is regulated in an experience-dependent manner during glomerular microcircuit maturation. Although different mechanisms are involved, these findings indicate that in the GL, the functional status of neuronal as well as astroglial gap junction channels is controlled by sensory inputs.

The local environment likely plays an important role in the GJC modulation observed in our study. Accordingly, astrocyte activity-dependent V_m fluctuations indicate that neuronal activity and $[K^+]_e$ variations might be important within OG, where the surrounding glial envelop is thought to limit K^+ spread (30). Moreover, the high level of Cx expression—in particular, Cx30—at the core of the OG where neuronal transmission occurs can also account for the GJC modulation by neuronal activity observed within OG.

Two Connexins, Two Distributions, Two Functions. Connexin immunostaining analysis demonstrates that Cx30 and Cx43 distributions are not similar. First, Cx30 is enriched in the GL compared with other OB layers (31) (*SI Appendix*, Fig. S1), suggesting a functional role prominent in this area. Second, within OG, Cx30 is highly expressed in the center, whereas Cx43 is mostly detected at the periphery, close to astrocyte cell bodies. Interestingly, our study shows that Cx30 is the molecular target for the activity dependency of OG astroglial networks, because both TTX treatment and early olfactory deprivation had no effect on glomerular astrocyte GJC in KO Cx30 mice. Cx30 location, in the central core of the OG, might be critical to fulfill this function. Moreover, this observation is also in agreement with the reported increase in Cx30 gene expression in brain of mice raised in an enriched environment (32). Together, these results obtained in OB slices suggest that glomerular astroglial networks are sustained by Cxs having two distinct functions: Cx30 supporting their plasticity and Cx43 whose channels are insensitive to neuronal activity.

Potassium Is a Key Element in Glomerular Neuroglial Interactions. Astrocyte V_m fluctuations recorded in OB slices are highly similar to those observed in vivo in cortical astrocytes (16). Because these cells express a high level of K^+ channels (33), V_m fluctuations mostly reflect variations in $[K^+]_e$ linked to neuronal activity (22). Based on these elements, we made the hypothesis that $[K^+]_e$ could be involved in the activity dependence of glomerular astroglial networks. Accordingly, we observed that high $[K^+]_e$ potentiates GJC between OG astrocytes, as shown in previous studies performed with cultured astrocytes (23, 24), but not in

Cx30 KO. In addition, high $[K^+]_e$ is also able to restore the level of coupling in the presence of TTX or after early sensory deprivation. Interestingly, when K_{ir} channels are blocked in astrocytes, GJC is inhibited, though neuronal activity is increased.

In summary, our findings indicate that glomerular astrocytes can detect changes in $[K^+]_e$ generated by neuronal activity through their K_{ir} channels and accordingly adapt their level of GJC. For many years, the primary function attributed to gap junctions in glia was their contribution to K^+ homeostasis during neuronal activity (34), a mechanism called K^+ buffering. Moreover, a modeling study has shown that the GJC between astrocytes is 5× more likely to support the K^+ transport than the extracellular diffusion (35). In the OG, this well-known property of K^+ buffering could support neuronal activity, a mechanism boosted by the K^+ itself via its facilitating effect on Cx30-mediated GJC between astrocytes. By favoring the fidelity of information transfer, this neuroglial loop of interactions may have an important impact on the first relay of olfactory information processing occurring at the glomerular level.

Methods

Experimental protocols were approved by Institut National de la Santé et de la Recherche Médicale health guidelines. Horizontal olfactory bulb slices (250–350 μm) were prepared from 5- to 25-d-old mice as previously described (17). All recordings were done at room temperature and according to previously described protocols (36). Details for electrophysiology, immunohistochemistry, and imaging and recording analysis are included in *SI Appendix, SI Methods*. For some experiments, the right naris was occluded by cauterization on P1 as recently described (29) to prevent stimuli from reaching the olfactory epithelium.

For each data group, results are expressed as mean ± SEM, and *n* refers to the number of independent experiments. Unless noted otherwise, unpaired two-tailed Student *t* test was used. Differences are considered significant at $*P < 0.05$, $**P < 0.01$, and $***P < 0.001$.

ACKNOWLEDGMENTS. The authors thank Drs. A. Koulakoff, N. Rouach, H. Gurden, and C. Martin for helpful discussions and P. Ezan for technical help. Support for this work was provided by a PhD fellowship from the Neuropôle de Recherche Francilien, Région Ile-de-France (to L.R.) and an Attaché Temporaire d'Enseignement et de Rechereche (ATER) position at the Collège de France. Support was also provided by Institut National de la Santé et de la Recherche Médicale and L'Agence Nationale de la Recherche Grant ANR-06-NEURO-004-01.

1. Mori K, Nagao H, Yoshihara Y (1999) The olfactory bulb: Coding and processing of odor molecule information. *Science* 286:711–715.
2. Mombaerts P, et al. (1996) Visualizing an olfactory sensory map. *Cell* 87:675–686.
3. Lancet D, Greer CA, Kauer JS, Shepherd GM (1982) Mapping of odor-related neuronal activity in the olfactory bulb by high-resolution 2-deoxyglucose autoradiography. *Proc Natl Acad Sci USA* 79:670–674.
4. Rubin BD, Katz LC (1999) Optical imaging of odorant representations in the mammalian olfactory bulb. *Neuron* 23:499–511.
5. Giaume C, Koulakoff A, Roux L, Holcman D, Rouach N (2010) Astroglial networks: A step further in neuroglial and gliovascular interactions. *Nat Rev Neurosci* 11:87–99.
6. Halassa MM, Haydon PG (2010) Integrated brain circuits: Astrocytic networks modulate neuronal activity and behavior. *Annu Rev Physiol* 72:335–355.
7. Bailey MS, Shipley MT (1993) Astrocyte subtypes in the rat olfactory bulb: Morphological heterogeneity and differential laminar distribution. *J Comp Neurol* 328: 501–526.
8. Chiu K, Greer CA (1996) Immunocytochemical analyses of astrocyte development in the olfactory bulb. *Brain Res Dev Brain Res* 95:28–37.
9. De Saint Jan D, Westbrook GL (2005) Detecting activity in olfactory bulb glomeruli with astrocyte recording. *J Neurosci* 25:2917–2924.
10. Doengi M, et al. (2009) GABA uptake-dependent Ca(2+) signaling in developing olfactory bulb astrocytes. *Proc Natl Acad Sci USA* 106:17570–17575.
11. Gurden H, Uchida N, Mainen ZF (2006) Sensory-evoked intrinsic optical signals in the olfactory bulb are coupled to glutamate release and uptake. *Neuron* 52:335–345.
12. Petzold GC, Albeanu DF, Sato TF, Murthy VN (2008) Coupling of neural activity to blood flow in olfactory glomeruli is mediated by astrocytic pathways. *Neuron* 58: 897–910.
13. Chaigneau E, et al. (2007) The relationship between blood flow and neuronal activity in the rodent olfactory bulb. *J Neurosci* 27:6452–6460.
14. Nolte C, et al. (2001) GFAP promoter-controlled EGFP-expressing transgenic mice: A tool to visualize astrocytes and astrogliosis in living brain tissue. *Glia* 33:72–86.
15. Regan MR, et al. (2007) Variations in promoter activity reveal a differential expression and physiology of glutamate transporters by glia in the developing and mature CNS. *J Neurosci* 27:6607–6619.
16. Mishima T, Hirase H (2010) In vivo intracellular recording suggests that gray matter astrocytes in mature cerebral cortex and hippocampus are electrophysiologically homogeneous. *J Neurosci* 30:3093–3100.
17. De Saint Jan D, Hirnet D, Westbrook GL, Charpak S (2009) External tufted cells drive the output of olfactory bulb glomeruli. *J Neurosci* 29:2043–2052.
18. Carlson GC, Shipley MT, Keller A (2000) Long-lasting depolarizations in mitral cells of the rat olfactory bulb. *J Neurosci* 20:2011–2021.
19. Philpot BD, Foster TC, Brunjes PC (1997) Mitral/tufted cell activity is attenuated and becomes uncoupled from respiration following naris closure. *J Neurobiol* 33:374–386.
20. Baker H (1990) Unilateral, neonatal olfactory deprivation alters tyrosine hydroxylase expression but not aromatic amino acid decarboxylase or GABA immunoreactivity. *Neuroscience* 36:761–771.
21. Kunzelmann P, et al. (1999) Late onset and increasing expression of the gap junction protein connexin30 in adult murine brain and long-term cultured astrocytes. *Glia* 25: 111–119.
22. Amzica F, Massimini M, Manfridi A (2002) Spatial buffering during slow and paroxysmal sleep oscillations in cortical networks of glial cells in vivo. *J Neurosci* 22: 1042–1053.
23. Enkvist MO, McCarthy KD (1994) Astroglial gap junction communication is increased by treatment with either glutamate or high K+ concentration. *J Neurochem* 62: 489–495.
24. De Pina-Benabou MH, Srinivas M, Spray DC, Scemes E (2001) Calmodulin kinase pathway mediates the K+-induced increase in Gap junctional communication between mouse spinal cord astrocytes. *J Neurosci* 21:6635–6643.
25. Houades V, Koulakoff A, Ezan P, Seif I, Giaume C (2008) Gap junction-mediated astrocytic networks in the mouse barrel cortex. *J Neurosci* 28:5207–5217.
26. Houades V, et al. (2006) Shapes of astrocyte networks in the juvenile brain. *Neuron Glia Biol* 2:3–14.
27. Marrero H, Orkand RK (1996) Nerve impulses increase glial intercellular permeability. *Glia* 16:285–289.
28. Rouach N, Glowinski J, Giaume C (2000) Activity-dependent neuronal control of gap-junctional communication in astrocytes. *J Cell Biol* 149:1513–1526.
29. Maher BJ, McGinley MJ, Westbrook GL (2009) Experience-dependent maturation of the glomerular microcircuit. *Proc Natl Acad Sci USA* 106:16865–16870.
30. Goriely AR, Secomb TW, Tolbert LP (2002) Effect of the glial envelope on extracellular K(+) diffusion in olfactory glomeruli. *J Neurophysiol* 87:1712–1722.
31. Nagy JI, Patel D, Ochalski PA, Stelmack GL (1999) Connexin30 in rodent, cat and human brain: Selective expression in gray matter astrocytes, co-localization with connexin43 at gap junctions and late developmental appearance. *Neuroscience* 88: 447–468.
32. Rampon C, et al. (2000) Effects of environmental enrichment on gene expression in the brain. *Proc Natl Acad Sci USA* 97:12880–12884.
33. Verkhratsky A, Steinhäuser C (2000) Ion channels in glial cells. *Brain Res Brain Res Rev* 32:380–412.
34. Kuffler SW, Nicholls JG, Orkand RK (1966) Physiological properties of glial cells in the central nervous system of amphibia. *J Neurophysiol* 29:768–787.
35. Gardner-Medwin AR (1983) A study of the mechanisms by which potassium moves through brain tissue in the rat. *J Physiol* 335:353–374.
36. Rouach N, Koulakoff A, Abudara V, Willecke K, Giaume C (2008) Astroglial metabolic networks sustain hippocampal synaptic transmission. *Science* 322:1551–1555.